

Articles

Diffuse Diffraction from Parallel/Antiparallel Metallocene Pillars

Levi J. Irwin, Paul D. Zeits, Joseph H. Reibenspies, and Stephen A. Miller*

Department of Chemistry, Texas A&M University, College Station, Texas 77843-3255

Received May 18, 2006

X-ray diffraction analyses of dimethyl *ansa*-metallocenes $(\text{CH}_3)_2\text{C}(\text{C}_5\text{H}_4)(\text{C}_{29}\text{H}_{36})\text{M}(\text{CH}_3)_2$ ($\text{M} = \text{Zr}$ or Hf) have revealed diffuse diffraction bands in the $0kl$ and $h0l$ single-crystal reciprocal lattice images, but not in the $hk0$ plane. This is consistent with metallic disorder in two dimensions and constitutes a rare example of diffuse diffraction for an organometallic compound. The metal is apparently partitioned between two sites with a 60:40 occupancy ratio. Structural interpretation of the X-ray data is consistent with a 60:40 ratio of parallel/antiparallel ($+z$, $-z$) metallocene pillars dispersed in the $x-y$ directions. Diffuse diffraction—albeit weaker—is also observed for the half-metallocene $(\text{C}_{29}\text{H}_{37})\text{Mn}(\text{CO})_3$, which occupies parallel/antiparallel pillars in an 80:20 ratio.

Introduction

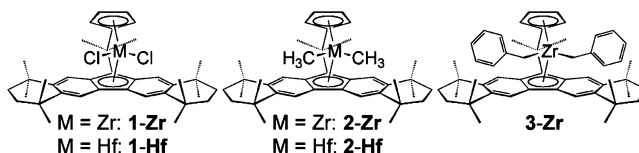
Diffuse X-ray diffraction is a somewhat common occurrence in the field of inorganic materials chemistry.¹ This phenomenon typically arises in ionic crystals or alloys because of disorder present in the crystal that can be characterized in real space as attributable to point defects, line defects, planar defects, and three-dimensional defects.² Likewise, diffuse diffraction is also somewhat common in organic molecular crystals,³ with substitutional and orientational disorder giving rise to defects in the molecular lattice.¹ However, diffuse diffraction is not as well documented in the realm of organometallic chemistry⁴ possibly because a ubiquitous goal (and prevalent outcome) in this field is the synthesis of discrete molecular species that are homogeneous in solution and retain their structural uniformity in the solid state.

In our ongoing research of dimensionally expansive (> 1 nm) organometallic complexes, we have identified and investigated an *ansa*-metallocene that displays conventional solution behavior, but apparently loses its structural homogeneity in the solid state, as evidenced by diffuse X-ray scattering phenomena associated with a disordered placement of the transition metal. The disorder is reconciled by an unprecedented arrangement

of organometallic pillars observed for both the zirconocene and hafnocene in the solid state.

Results and Discussion

The octamethyloctahydrodibenzofluorenyl ligand is a sterically expanded version of the fluorenyl ligand (14 vs 9 Å), which has recently been incorporated into metallocene dichlorides $(\text{CH}_3)_2\text{C}(\text{C}_5\text{H}_4)(\text{C}_{29}\text{H}_{36})\text{MCl}_2$ of zirconium (**1-Zr**) and hafnium (**1-Hf**). This simple steric modification generally results in markedly increased activity and syndioselectivity in the MAO-cocatalyzed (MAO = methylaluminoxane) polymerization of propylene.⁵ Pursuant to the study of these and related catalytic enhancements offered by the octamethyloctahydrodibenzofluorenyl ligand,⁶ derivative dimethyl metallocenes $(\text{CH}_3)_2\text{C}(\text{C}_5\text{H}_4)(\text{C}_{29}\text{H}_{36})\text{M}(\text{CH}_3)_2$ (**2-Zr**, **2-Hf**) and the dibenzyl metallocene $(\text{CH}_3)_2\text{C}(\text{C}_5\text{H}_4)(\text{C}_{29}\text{H}_{36})\text{Zr}(\text{CH}_2\text{C}_6\text{H}_5)_2$ (**3-Zr**) were synthesized.



Single-crystal X-ray diffraction studies of the isomorphous dichloro metallocenes (**1-Zr** and **1-Hf**) and the dibenzyl metallocene (**3-Zr**) reveal bonding modes (η^5, η^5) and solid-state packing motifs typical of bent metallocenes (Figure 1). However, the X-ray diffraction patterns from single crystals of the isomorphous *dimethyl* metallocenes **2-Zr** and **2-Hf** present bands attributable to diffuse diffraction phenomena, which are not well documented for organometallic species and constitute very distinct diffuse scattering band patterns, reports of which are scarce for this class of compound. The bands are observable

* To whom correspondence should be addressed. E-mail: samiller@mail.chem.tamu.edu.

(1) Welberry, T. R.; Butler, B. D. *Chem. Rev.* **1995**, *95*, 2369–2403. (2) Jagadzinski, H. *Prog. Crystal Growth Charact.* **1987**, *14*, 47–102. (3) (a) Welberry, T. R. *Acta Crystallogr.* **2001**, *A57*, 244–255. (b) Welberry, T. R. *Acta Crystallogr.* **2000**, *A56*, 348–358. (c) Welberry, T. R.; Goossens, D. J.; Edwards, A. J.; David, W. I. F. *Acta Crystallogr.* **2001**, *A57*, 101–109. (d) Bürgi, H.-B.; Hostettler, M.; Birkedal, H.; Schwarzenbach, D. Z. *Kristallogr.* **2005**, *220*, 1066–1075.

(4) (a) The only apparent example for an organometallic single crystal is the polynuclear cluster compound $\text{Fe}_3(\text{CO})_{12}$. Welberry, T. R.; Proffen, T.; Bown, M. *Acta Crystallogr.* **1998**, *A54*, 661–674. (b) An organometallic thin film (with no long-range lateral order) has also displayed diffuse diffraction. Salditt, T.; Ana, Q.; Plech, A.; Peisl, J.; Eschbaumer, C.; Weidl, C. H.; Schubert, U. S. *Thin Solid Films* **1999**, *354*, 208–214. (c) Iodine-doped phthalocyanine compounds, having uranium–nitrogen or ytterbium–nitrogen bonds, are examples of coordination compounds exhibiting diffuse diffraction. Krawczyk, J.; Pietraszko, A.; Kubiak, R.; Lukaszewicz, K. *Acta Crystallogr.* **2003**, *B59*, 384–392.

(5) Miller, S. A.; Bercaw, J. E. *Organometallics* **2004**, *23*, 1777–1789.

(6) (a) Irwin, L. J.; Reibenspies, J. H.; Miller, S. A. *J. Am. Chem. Soc.* **2004**, *126*, 16716–16717. (b) Irwin, L. J.; Miller, S. A. *J. Am. Chem. Soc.* **2005**, *127*, 9972–9973. (c) Irwin, L. J.; Reibenspies, J. H.; Miller, S. A. *Polyhedron* **2005**, *24*, 1314–1324.

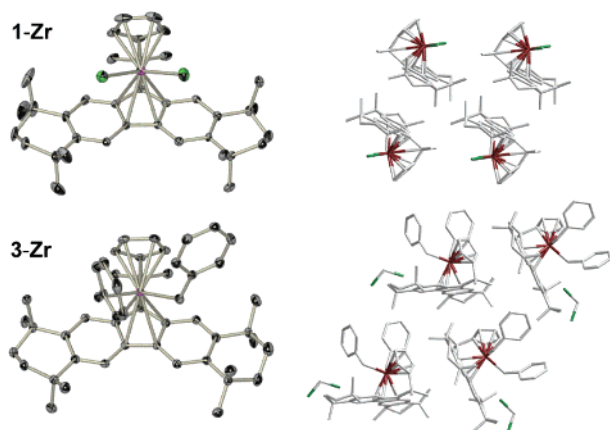


Figure 1. Single-crystal X-ray structures (with 50% probability ellipsoids; hydrogens omitted) and packing diagrams for **1-Zr** (**1-Hf** is isomorphic) and **3-Zr**·CH₂Cl₂.

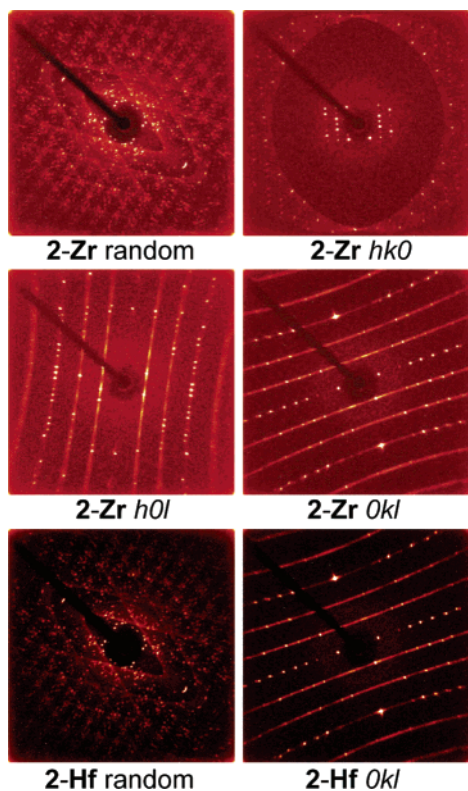


Figure 2. Single-crystal reciprocal lattice images of (CH₃)₂C-(C₅H₄)(C₂₉H₃₆)M(CH₃)₂ (**2-Zr** and **2-Hf**) showing random orientation and the *hk0*, *h0l*, and *Ok1* planes.

in the *Ok1* and *h0l* planes, but they are absent in the *hk0* plane (Figure 2); these observations are consistent with metallic disorder in two dimensions.⁷

Initial structure refinement of the diffraction data revealed that the metallocenes pack in pillars (Figure 3) and suggested the presence of two limiting pillared structures: one accounting for the conventional placement of the transition metal with 60% occupancy (Figure 4a) and another accounting for a second placement of the transition metal with 40% occupancy (Figure 4b). A hybrid pillar (Figure 4c), with an internally dis-

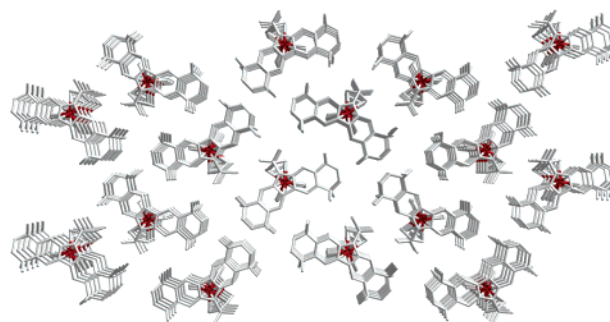


Figure 3. Parallel pillaring observed in **2-Zr** (and isomorphic **2-Hf**). Hydrogen atoms have been omitted for clarity.

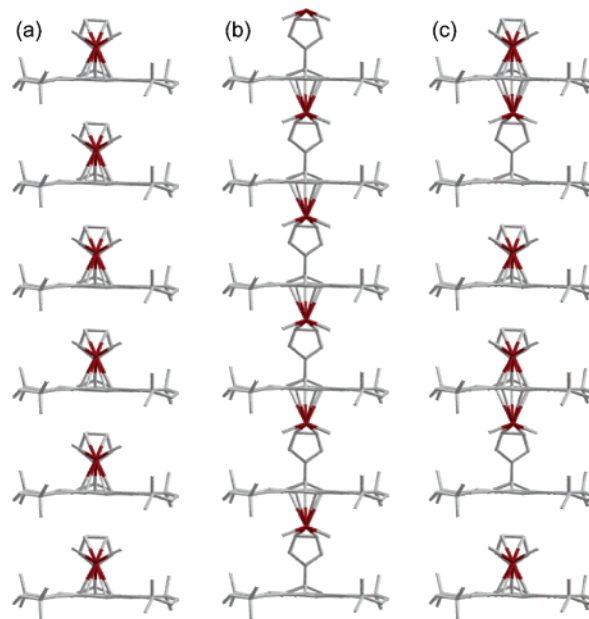


Figure 4. Possible extended pillar structures for **2-Zr** and **2-Hf** that account for placement of the transition metal in two positions in the crystal lattice (hydrogen atoms omitted). Structures b and c involve unconventional and disfavored bonding modes.

ordered transition metal arrangement, was deemed unlikely because it necessitates unfavorable charge separation at certain junctures.⁸

The unusual and unlikely η^2 -cyclopentadienyl bonding mode⁹ represented in Figure 4b—in which a metal spans two different ligands—prompted a reanalysis of the X-ray diffraction data. This time the pillars, which are directional, were allowed to propagate in either direction as dictated by a pseudomirror plane. This ameliorated the seemingly unfavorable bonding situations of Figure 4b and 4c, allowed the metals to occupy only the conventional position for a metallocene (η^5, η^5), and satisfyingly located the transition metal in two unique crystallographic positions, as mandated by the diffuse diffraction pattern. The resultant arrangement of the metallocene pillars is a 60:40 parallel/antiparallel configuration (Figure 5), dispersed in the *x-y* directions.

Additionally, analysis of the solid-state structure of octamethyloctahydrodibenzofluorene provides insight into the pro-

(8) Charge distribution calculations were performed with the semiempirical PM3 method. See the Supporting Information.

(9) (a) η^2 -Cyclopentadienyl complexes of tantalum have been reported. Chirik, P. J.; Zubris, D. L.; Ackerman, L. J.; Henling, L. M.; Day, M. W.; Bercaw, J. E. *Organometallics* **2003**, *22*, 172–187. (b) Chirik, P. J. Ph.D. Thesis, California Institute of Technology, 2000. (c) Zubris, D. L. Ph.D. Thesis, California Institute of Technology, 2001.

(7) (a) Daniels, P. J. *J. Appl. Crystallogr.* **1998**, *31*, 559–569. (b) Greber, T.; Osterwalder, J.; Schlapbach, L. *Springer Ser. Surface Sci.* **1991**, *24* (3), 355–359. (c) Dornberger-Schiff, K. *Acta Crystallogr.* **1964**, *17*, 482–491.

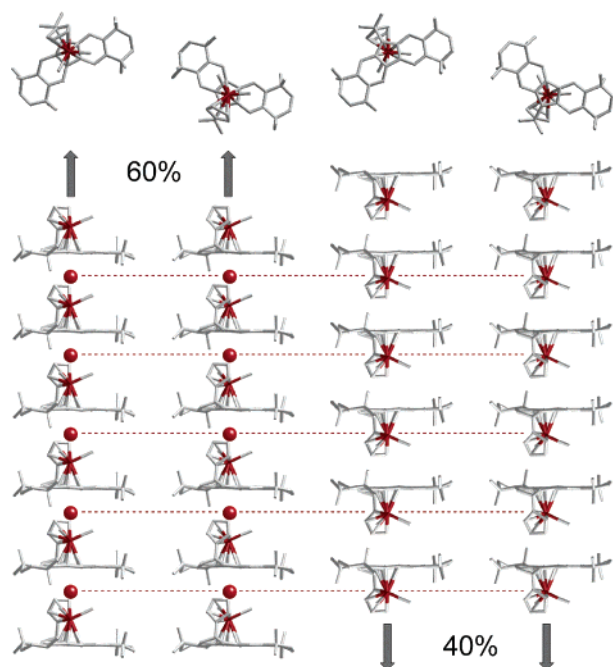


Figure 5. The best explanation for the diffuse diffraction of **2-Zr** and **2-Hf** is a 60:40 arrangement of parallel/antiparallel (+z, -z) pillars, dispersed in the x - y directions. This explains the 40% occupancy of the transition metal in the disordered position (shown by the red ball).

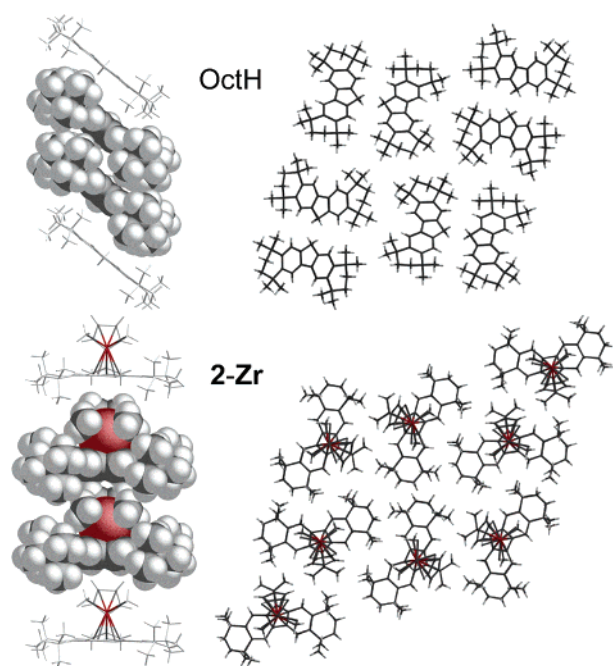


Figure 6. Packing diagrams of octamethyloctahydrodibenzofluorene (OctH) and **2-Zr** showing (1) occupancy of the voids above and below the aromatic plane and (2) similar packing arrangements of the pillars.

density of **2-Zr** and **2-Hf** to form pillared structures. The angular stacking in this nonplanar hydrocarbon allows each void to be filled by the tetramethyltetrahydrobenzo group of the next molecule (Figure 6). Similarly, the cyclopentadienyl- $M(\text{CH}_3)_2$ portion of one metallocene has commensurate size and polarity to occupy the void presented by the octamethyloctahydrodibenzofluorenyl ligand of the next metallocene, resulting in the occurrence of linear, organometallic pillaring.¹⁰

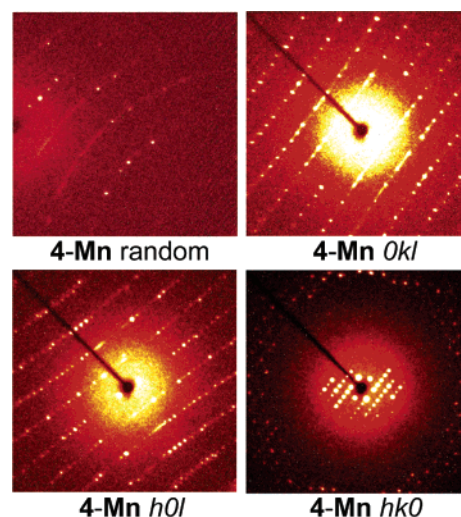


Figure 7. Single-crystal reciprocal lattice images of $(\text{C}_{29}\text{H}_{37})\text{Mn}(\text{CO})_3$ (**4-Mn**) showing random orientation and the $Ok\bar{l}$, $h0l$, and $hk0$ planes.

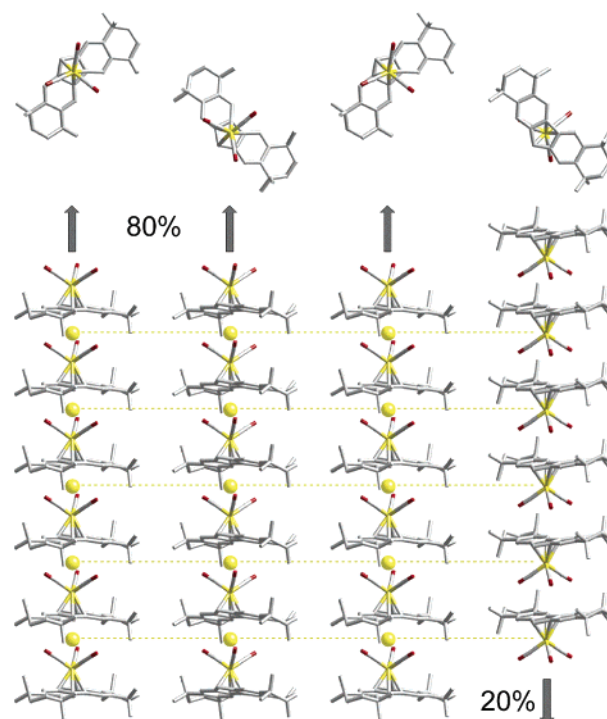


Figure 8. The best explanation for the diffuse diffraction of **4-Mn** is an 80:20 arrangement of parallel/antiparallel (+z, -z) pillars, dispersed in the x - y directions. This explains the 20% occupancy of the transition metal in the disordered position (shown by the yellow ball).

This diffuse diffraction phenomenon appears to be somewhat general, as it has been identified in a structurally related half-metallocene that contains the octamethyloctahydrodibenzofluorenyl ligand. Figure 7 depicts the diffuse diffraction bands found for $(\text{C}_{29}\text{H}_{37})\text{Mn}(\text{CO})_3$ (**4-Mn**), similarly found only in two dimensions ($Ok\bar{l}$ and $h0l$).¹¹ These bands are weaker than those seen with **2-Zr** and **2-Hf**. Solution refinement suggests an 80:20 partitioning of parallel/antiparallel pillars, which are readily formed by interlocking the $-\text{Mn}(\text{CO})_3$ moiety into the void of the next octamethyloctahydrodibenzofluorenyl ligand (Figure 8). The final refinement was obtained by assuming binary pillar up and pillar down disorder, again as dictated by a pseudomirror plane.

Conclusions

In summary, X-ray diffraction analyses of **2-Zr** and **2-Hf** have revealed unusual solid-state structures with organometallic pillaring. The diffuse diffraction bands observed suggest a 60:40 juxtaposition of parallel/antiparallel metallocene pillars to explain the 60:40 site occupancy of the disordered transition metal in the crystal. The two-dimensional metallic disorder provides one of the sharpest examples of X-ray diffuse diffraction known for any type of crystal. The related disorder of half-metallocene **4-Mn** provides weaker diffuse diffraction (80:20 parallel/antiparallel pillars), but implies that this phenomenon is general. In addition to structural novelty, these types of crystals offer an opportunity to further study the diffuse X-ray diffraction phenomenon in a molecularly defined crystal with simple, binary disorder.

Experimental Section

General Considerations. All air-sensitive procedures were performed under a purified atmosphere of nitrogen in a glovebox equipped with a $-35\text{ }^{\circ}\text{C}$ freezer or by using standard Schlenk line and vacuum line techniques.¹² Solvents were dried using standard procedures. 6,6-Dimethylfulvene,¹³ benzyl potassium,¹⁴ and octamethyloctahydrodibenzofluorene^{6a} were prepared according to literature procedures. Other reagents were used as received unless otherwise noted. All NMR chemical shifts are given in ppm and were recorded on a Mercury-300BB spectrometer (^1H , 299.91 MHz; $^{13}\text{C}\{^1\text{H}\}$, 75.41 MHz) using the solvent peak (or residual protonated solvent peak) as an internal standard (CDCl_3 , ^1H , 7.27 ppm; ^{13}C , 77.0 ppm; C_6D_6 , ^1H , 7.15 ppm; ^{13}C , 128.39 ppm).

Metallocene and Half-Metallocene Syntheses. The exemplary syntheses of **2-Zr** and **4-Mn** are given below. Complete synthetic details for the remaining compounds are found in the Supporting Information.

$(\text{CH}_3)_2\text{C}(\text{C}_5\text{H}_4)(\text{C}_{29}\text{H}_{36})\text{H}_2$. A 500 mL round-bottom flask was charged with octamethyloctahydrodibenzofluorene (20.00 g, 51.73 mmol), a 180° needle valve was attached, and the system was evacuated. Tetrahydrofuran (200 mL) was then vacuum transferred in followed by the addition of *n*-butyllithium (19.8 mL, 56.90 mmol, 2.87 M in hexanes) via syringe. After warming to room temperature, the red slurry was heated to $40\text{ }^{\circ}\text{C}$ and stirred for 30 min, after which the evolution of butane had ceased. 6,6-Dimethylfulvene (5.49 g, 51.73 mmol) was then syringed in. After 43.5 h, 75.0 mL of saturated NaCl solution was poured into the homogeneous red solution. The organic phase was separated from the aqueous phase and dried thoroughly with MgSO_4 and filtered, and the solvent was removed by rotary evaporation, leaving a white solid. This solid was recrystallized from boiling *n*-propanol, collected by filtration, and dried under high vacuum for 48 h. This yielded a snow-white, fluffy solid: 25.19 g (98.8%). ^1H NMR (CDCl_3): major isomer

(67%): δ 1.05 (s, 6H, isopropylidene CH_3), 1.21 (s, 6H, Oct- CH_3), 1.23 (s, 6H, Oct- CH_3), 1.35 (s, 6H, Oct- CH_3), 1.39 (s, 6H, Oct- CH_3), 1.70 (apparent s, 8H, Oct- CH_2), 3.11 (s, 2H, Cp- CH_2), 4.04 (s, 1H, Oct- CH_1), 5.93 (s, 1H, Cp- CH_1), 6.49 (m, 1H, Cp- CH_1), 6.67 (m, 1H, Cp- CH_1), 7.10 (s, 2H, Oct- CH_1), 7.57 (s, 2H, Oct- CH_1); minor isomer (33%): δ 1.07 (s, 6H, isopropylidene CH_3), 1.22 (s, 6H, Oct- CH_3), 1.25 (s, 6H, Oct- CH_3), 1.35 (s, 6H, Oct- CH_3), 1.39 (s, 6H, Oct- CH_3), 1.70 (apparent s, 8H, Oct- CH_2), 3.22 (s, 2H, Cp- CH_2), 3.99 (s, 1H, Oct- CH_1), 6.14 (s, 1H, Cp- CH_1), 6.56 (m, 1H, Cp- CH_1), 7.00 (m, 1H, Cp- CH_1), 6.97 (s, 2H, Oct- CH_1), 7.57 (s, 2H, Oct- CH_1). $^{13}\text{C}\{^1\text{H}\}$ NMR (CDCl_3): δ 24.48, 25.53, 31.78, 31.81, 32.18, 32.21, 34.36, 34.44, 35.2, 35.29, 35.34, 39.5, 40.5, 40.7, 41.0, 54.8, 57.3, 116.3, 116.4, 123.9, 124.1, 124.5, 126.3, 130.8, 132.4, 133.6, 133.9, 139.5, 139.6, 142.1, 142.2, 142.60, 142.64, 143.2, 143.3, 155.9, 158.4. APCI+: m/z 491.2 ($\text{M} - \text{H}$)⁺.

$(\text{CH}_3)_2\text{C}(\text{C}_5\text{H}_4)(\text{C}_{29}\text{H}_{36})\text{ZrCl}_2$ (1-Zr**).** A 200 mL round-bottom flask was charged with $(\text{CH}_3)_2\text{C}(\text{C}_5\text{H}_4)(\text{C}_{29}\text{H}_{36})\text{H}_2$ (15.00 g, 30.44 mmol) and attached to a 3 cm swivel frit. This was then evacuated, and 100 mL of diethyl ether was vacuum transferred in. Next, *n*-butyllithium (23.3 mL, 66.97 mmol, 2.87 M in hexanes) was syringed in. The solution exhibited two events. The first event was fast and exothermic, while the second was a slow color change from yellow to orange and finally red. After 17 h an orange precipitate was observed. After a total of 64.5 h, the ether was removed under vacuum and ZrCl_4 (7.09 g, 30.44 mmol) was added in the glovebox. The frit was again evacuated, and diethyl ether (40 mL) was vacuum transferred in. The product was extracted after 51 h, the resulting slurry was concentrated, and the product was collected as a dark red cake on the frit. It was washed three times with the ether, removing an orange, oily substance. The red solid was then dried under vacuum to yield pure product: 11.69 g (58.8%). Large, red, needle-like crystals suitable for X-ray diffraction can be grown by vapor diffusion of diethyl ether into a saturated dichloromethane solution. ^1H NMR (CDCl_3): δ 1.27 (s, 6H, Oct- CH_3), 1.40 (s, 6H, Oct- CH_3), 1.43 (s, 6H, Oct- CH_3), 1.54 (s, 6H, Oct- CH_3), 1.76 (apparent s, 8H, Oct- CH_2), 2.35 (s, 6H, isopropylidene CH_3), 5.58 (m, 2H, Cp- CH_1), 6.27 (m, 2H, Cp- CH_1), 7.65 (s, 2H, Oct- CH_1), 8.04 (s, 2H, Oct- CH_1). $^{13}\text{C}\{^1\text{H}\}$ NMR (CDCl_3): δ 28.7, 32.2, 32.5, 32.6, 33.8, 34.7, 34.8, 35.0, 35.1, 40.0, 75.0, 100.2, 112.8, 118.4, 120.3, 121.0, 121.4, 122.1, 145.5, 147.5.

$(\text{CH}_3)_2\text{C}(\text{C}_5\text{H}_4)(\text{C}_{29}\text{H}_{36})\text{Zr}(\text{CH}_3)_2$ (2-Zr**).** A 200 mL recovery flask was charged with **1-Zr** (4.00 g, 6.13 mmol). To this was added 160 mL of toluene, giving a nearly homogeneous red solution. Next, CH_3MgCl (4.84 mL, 12.87 mmol, 2.66 M in tetrahydrofuran) was syringed in, yielding an initially red, and then orange, and finally bright yellow solution. The MgCl_2 was removed by filtration, and the toluene was removed under high vacuum. Next, 50 mL of diethyl ether was vacuum transferred in, and the yellow slurry was triturated for 30 min, after which time the volume was reduced to 20 mL and the yellow solid was isolated by filtration. The yellow cake was washed once with about 5 mL of diethyl ether and then dried under vacuum. The yellow solid was then recrystallized from boiling 1,2-dimethoxyethane, and two crops were collected, yielding 2.17 g (57.9%). Yellow, needle-like crystals suitable for X-ray diffraction were grown from cooling a saturated dichloromethane solution to $-35\text{ }^{\circ}\text{C}$ and also by vapor diffusion of diethyl ether into a saturated dichloromethane solution. ^1H NMR (CDCl_3): δ -1.58 (s, 6H, Zr- CH_3), 1.27 (s, 6H, Oct- CH_3), 1.40 (s, 6H, Oct- CH_3), 1.47 (s, 6H, Oct- CH_3), 1.51 (s, 6H, Oct- CH_3), 1.77 (m, 8H, Oct- CH_2), 2.14 (s, 6H, isopropylidene CH_3), 5.44 (m, 2H, Cp- CH_1), 6.24 (m, 2H, Cp- CH_1), 7.57 (s, 2H, Oct- CH_1), 8.12 (s, 2H, Oct- CH_1). $^{13}\text{C}\{^1\text{H}\}$ NMR (CDCl_3): δ 28.9, 30.8, 32.55, 32.6, 32.9, 33.8, 34.5, 35.0, 35.1, 35.2, 39.7, 72.1, 99.8, 108.0, 112.3, 117.9, 119.6, 120.8, 123.0, 141.3, 145.2.

$(\text{C}_{29}\text{H}_{37})\text{Li}$. In a nitrogen-filled glovebox, octamethyloctahydrodibenzofluorene (4.133 g, 10.69 mmol) was dissolved in toluene

(10) (a) Tsvetkov, F.; White, J. *J. Am. Chem. Soc.* **1988**, *110*, 3183–3187. (b) Tsvetkov, F.; White, J. *Chem. Mater.* **1989**, *1*, 149–158. (c) Munakata, M.; Wu, L. P.; Ning, G. L.; Kuroda-Sowa, T.; Maekawa, M.; Suenaga, Y.; Maeno, N. *J. Am. Chem. Soc.* **1999**, *121*, 4968–4976. (d) Gil, A.; Gandia, L. M.; Vicente, M. A. *Cat. Rev.-Sci. Eng.* **2000**, *42*, 145–212. (e) Masciocchi, N.; Sironi, A.; Chardon-Noblat, S.; Deronzier, A. *Organometallics* **2002**, *21*, 4009–4012. (f) Chui, S. S. Y.; Ng, M. F. Y.; Che, C.-M. *Chem.-Eur. J.* **2005**, *11*, 1739–1749. (g) Calvo-Perez, V.; Vega, A.; Spodine, E. *Organometallics* **2006**, *25*, 1953–1960.

(11) The fluorene-based half-metallocene $(\text{C}_{13}\text{H}_6)\text{Mn}(\text{CO})_3$ is known, but does not exhibit pillaring or diffuse diffraction. Decken, A.; MacKay, A. J.; Brown, M. J.; Bottomley, F. *Organometallics* **2002**, *21*, 2006–2009.

(12) Burger, B. J.; Bercaw, J. E. In *Experimental Organometallic Chemistry: A Practicum in Synthesis and Characterization*; Wayda, A. L., Darensbourg, M. Y., Eds.; American Chemical Society: Washington, DC, 1987; Vol. 357, pp 79–98.

(13) Stone, K. J.; Little, R. D. *J. Org. Chem.* **1984**, *49*, 1849–1853.

(14) Schlosser, M.; Hartmann, J. *Angew. Chem., Int. Ed. Engl.* **1973**, *12*, 508–509.

Table 1. Crystal Data and Refinement Details for Diffuse Diffracting Crystals

	2-Zr	2-Hf	4-Mn
empirical formula	C ₃₉ H ₅₂ Zr	C ₃₉ H ₅₂ Hf	C ₃₂ H ₃₇ O ₃ Mn
fw	612.03	699.30	524.56
temperature (K)	110(2)	110(2)	110(2)
wavelength (Å)	1.54178	0.71073	0.71073
cryst syst	orthorhombic	orthorhombic	orthorhombic
space group	<i>Pna</i> 2 ₁	<i>Pna</i> 2 ₁	<i>Pna</i> 2 ₁
<i>a</i> (Å)	29.750(6)	29.775(5)	26.234(7)
<i>b</i> (Å)	14.980(3)	15.007(2)	16.479(5)
<i>c</i> (Å)	7.3554(17)	7.3342(12)	6.3671(18)
α (deg)	90	90	90
β (deg)	90	90	90
γ (deg)	90	90	90
volume (Å ³)	3277.9(12)	3277.3(9)	2752.5(13)
<i>Z</i>	4	4	4
density (calc, gcm ⁻³)	1.240	1.417	1.266
μ (mm ⁻¹)	2.909	3.208	0.510
cryst size (mm ³)	0.10 × 0.10 × 0.10	0.40 × 0.20 × 0.20	0.20 × 0.10 × 0.05
2-θ, <i>R</i> (int)	118.36°, 0.0792	55.06°, 0.0517	50.88°, 0.0935
no. of reflns	17 192	22 973	19 867
no. of indep reflns	4520	5349	4728
no. of data/restraints/params	4520/1257/723	5349/1613/723	4728/525/471
GOF (<i>F</i> ²)	1.008	1.056	1.036
<i>R</i> ₁ [<i>I</i> > 2σ(<i>I</i>)]	0.0858	0.0830	0.0730
<i>wR</i> ₂ [<i>I</i> > 2σ(<i>I</i>)]	0.1692	0.1852	0.1706
<i>R</i> ₁ (all data)	0.1029	0.0847	0.0934
<i>wR</i> ₂ (all data)	0.1785	0.1866	0.1845
largest diff peak, hole (e Å ⁻³)	0.785, -0.776	2.598, -2.581	0.391, -0.483
metal occupancy ratio	58.6:41.4	62.8:37.2	79.5:20.5

(50 mL), and *n*-butyllithium (5.13 mL of a 2.5 M solution in hexanes, 13 mmol) was added via syringe. The flask was attached to a swivel frit, and the apparatus was affixed to the vacuum line. After heating to 75 °C for 14 h, the precipitated solid was collected by filtration. Drying *in vacuo* afforded the pink product in 97.0% yield (4.07 g).

(C₂₉H₃₇)Mn(CO)₃ (4-Mn). In a nitrogen-filled glovebox, (C₂₉H₃₇)-Li (786 mg, 2.00 mmol) and BrMn(CO)₅ (550 mg, 2.0 mmol) were combined in a 100 mL receiving flask and sealed with a 180° needle valve. The flask was then evacuated on the vacuum line, and THF (50 mL) was condensed in at 77 K. The reaction was slowly warmed to room temperature and stirred for 24 h, at which time the solvent was removed *in vacuo*. The resulting yellow solid was extracted into pentane (60 mL) and filtered through a pad of Celite inside a swivel frit. Concentration to 20 mL and stirring overnight afforded the title compound as a yellow powder. The precipitated solid was then collected by filtration, washed with pentane, and dried *in vacuo* to yield 180 mg. A second crop is obtained from subsequent concentration of the filtrate to 6 mL to yield 319 mg. The yield for two crops is 499 mg (47.6%). Yellow, needle-like crystals suitable for X-ray diffraction were grown from a saturated solution in pentane undergoing slow evaporation into a surrounding solution of toluene at -35 °C. Crystals can also be grown by cooling a saturated solution in pentane to -35 °C. ¹H NMR (C₆D₆): δ 1.21 (s, 6H, Oct-CH₃), 1.23 (s, 6H, Oct-CH₃), 1.29 (s, 6H, Oct-CH₃), 1.30 (s, 6H, Oct-CH₃), 1.52 (apparent s, 8H, Oct-CH₂), 5.22 (s, 1H, Oct-CH₁), 7.33 (s, 2H, Oct-CH₁), 8.09 (s, 2H, Oct-CH₁). ¹³C {¹H} NMR (C₆D₆): δ 32.7, 32.92, 32.94, 33.0, 35.36, 35.36, 35.40, 35.5, 58.2, 95.5, 106.3, 121.6, 122.4, 144.0, 147.5, 227.1.

X-ray Crystallography. Crystals were mounted at room temperature in mineral oil and affixed to a nylon fiber. X-ray crystallographic data were obtained using a Bruker SMART 1000 three-circle diffractometer operating at 50 kV and 40 mA, Mo Kα

(λ = 0.71073 Å) with a graphite monochromator and a CCD detector or a Bruker GADDS instrument operating at 40 kV and 40 mA, Cu Kα (λ = 1.54578 Å) with a graphite monochromator and a CCD detector. Details of the crystallographic data collection and refinement for diffuse diffracting crystals are summarized in Table 1. The molecular structures were solved by direct methods and were refined employing the SHELXS-97 and SHELXL-97 programs.¹⁵ For **2-Zr**, **2-Hf**, and **4-Mn**, the average structure was modeled by placement of two full molecular structures that were related by a pseudomirror plane, near the same positions in real space. The two disordered structures were refined by full molecular disorder procedures. Finally, an inverse twin refinement (final BASF parameters were 0.27, 0.30, and 0.10 for **2-Zr**, **2-Hf**, and **4-Mn**, respectively) was employed and the disordered model was refined to convergence.

Acknowledgment. This research is supported by grants from The Robert A. Welch Foundation (No. A-1537) and the Texas Advanced Technology Program (No. 010366-0196-2003). The National Science Foundation (CAREER CHE-0548197) is also graciously acknowledged for financial support. The authors are indebted to Professor Gerard Parkin for insightful structural and crystallographic discussions.

Supporting Information Available: Experimental procedures and compound characterization data, including X-ray crystallographic data for **1-Zr**, **1-Hf**, **2-Zr**, **2-Hf**, **3-Zr**, **4-Mn**, and octamethyloctahydrodibenzofluorene. This material is available free of charge via the Internet at <http://pubs.acs.org>.

OM060435G

(15) (a) Sheldrick, G. M. *SHELXS-97*, program for the solution of crystal structures; Universität Göttingen, 1997. (b) Sheldrick, G. M. *SHELXL-97*, program for the solution of crystal structures; Universität Göttingen, 1997.